Supplementary Data

Methods

Measurement of reactive oxygen species using DCFDA fluorescence

Angiotensin II (Ang II-) and H_2O_2-induced reactive oxygen species (ROS) generation in human H295R cells and rat adrenal cortex was monitored by fluorescence microscopy. Cells and fresh adrenal cortical sections (20 μm) were loaded with 5 μM 6-Carboxy- 2′,7′-dichlorodihydrofluorescein diacetate (DCFDA) in basal DME/Ham's F-12 medium for 30 min at 37°C in a 5% air–5% CO_2 environment. After DCFDA loading, cells and tissue sections were treated with Dulbecco's modified Eagle's medium containing Ang II (1–1000 nM) for a duration as indicated in the figure S2. At the end of the incubation, cells and tissue sections were washed twice with warm phosphate-buffered saline (PBS) and examined under a Zeiss Axiovert100TV inverted fluorescence microscope using excitation and emission wavelengths of 495 and 520 nm, respectively. Images were captured on a high-resolution, cooled CCD camera system using a 20× objective lens. The fields were randomly selected for imaging, and statistical analyses were performed by Image J software (Wayne Rasband).

In experiments assessing the effects of various reagents such as antioxidants and Nox inhibitor, cells and tissue sections were pretreated with optimal concentrations of respective reagents (as established in preliminary experiments) for 30 min before DCFDA loading and treatment with either Ang II or H_2O_2 as just described.

Measurement of mitochondrial ROS

Mitochondrial ROS was measured using MitoSOX Red (3,8-phenanthridinediamine, 5-(6′-Triphenylphosphonium-hexyl)-5,6 dihydro-6-phenyl), and following the protocol provided by the manufacturer. Briefly, three groups of H295R cells were examined: untreated, Ang-II (10 nM)-treated, and antimycin A (100 μM)-treated cells (positive control). The digital images were taken by an inverted confocal laser scanning microscope (Leica SP5 II STED-CW System) at 2048×2048 pixels using an argon laser excitation at 510 nm with emission collection through a 580-nm long-pass filter as previously described (6, 9). Images were captured using 63× oil immersion objective lens, and the optical section was <1 μm.

Immunohistochemistry

Immunostaining for aldosterone synthase (CYP11B2) was performed in human H295R cells and freshly isolated unfixed rat adrenal cortical sections. Cells were treated with either vehicle (control) or Ang II (10 nM) in the absence and presence of various reagents for 6 h at 37°C in a 95% air–5% CO_2 environment. In addition, in parallel experiments, cells were treated with either vehicle (control) or H_2O_2 (50 nM) in the absence and presence of H_2O_2 scavenger (PEG-Catalase, 350 U/ml). Adrenal glands were harvested from Sprague-Dawley rats, and a free-floating section (20 μm) containing the zona glomerulosa region of the cortex was treated with Ang II (100 nM for 6 h) alone or in the presence of the Nox inhibitor (VAS-2870, 20 μM). After treatments, both cells and adrenal cortical sections were sequentially treated with reagents as described next wherein before each step, they were rinsed with PBS. The treatments include (i) 3.7% formaldehyde in PBS for 10 min (fixation); (ii) 0.1% Triton X-100 in PBS for 5 min (permeabilization); (iii) 10% donkey serum in PBS for 30 min (blocking nonspecific binding sites); (iv) either goat anti-CYP11B2 antibody (1:100 dilution; Santa Cruz Biotechnology) (for H295R cells) or mouse anti-CYP11B2 antibody (1:50 dilution; Millipore) (for rat adrenal cortex) in PBS containing either 1% donkey or goat serum overnight at 4°C (primary); (v) either Alexa Fluor 488 conjugated donkey anti-goat antibody (1:1000 dilution; Molecular Probes) (for H295R cells) or Alexa Fluor 555 conjugated goat anti-mouse antibody (1:1000 dilution; Molecular Probes) (for rat adrenal cortex) in PBS for 1 h at room temperature (secondary). Sections treated with only secondary antibody were used as negative controls. Slides were prepared with mounting medium containing 4′, 6-diamidino-2-phenylindole (Vector Laboratories) for nuclear staining. Confocal images were captured using a 63× numerical aperture oil objective on a Leica SP5 II STED-CW System with identical gain settings between samples using Leica software (Exton).

Measurement of aconitase activity

Mitochondrial fractions were isolated from H295R cell extracts by differential centrifugation (4). Aconitase activity was determined in these fractions as previously described (1) and expressed as micromoles of isocitrate per minute per milligram of protein.

References

1. Gardner PR, Raineri I, Epstein LB, and White CW. Superoxide radical and iron modulate aconitase activity in mammalian cells. *J Biol Chem* 270: 13399–13405, 1995.
2. Harper RW, Xu C, Eiserich JP, Chen Y, Kao CY, Thai P, Setiadi H, and Wu R. Differential regulation of dual NADPH oxidases/peroxidases, Duox1 and Duox2, by Th1 and Th2 cytokines in respiratory tract epithelium. *FEBS Lett* 29: 4911–4917, 2005.
3. Huang XJ, Ihsan A, Wang X, Dai MH, Wang YL, Su SJ, Xue XJ, and Yuan ZH. Long-term dose-dependent response of Mequindox on aldosterone, corticosterone and five steroidogenic enzyme mRNAs in the adrenal of male rats. *Toxicol Lett* 191: 167–173, 2009.
4. Lai JC and Clark JB. Preparation of synaptic and non-synaptic mitochondria from mammalian brain. *Methods Enzymol* 55: 51–60, 1979.
5. MacKenzie SM, Dewar D, Stewart W, Fraser R, Connell JMC, and Davies E. The transcription of steriodogenic genes in the human cerebellum and hippocampus: a comparative survey of normal and Alzheimer's tissue. *J Endocrinol* 196: 123–130, 2008.
6. Mukhopadhyay P, Rajesh M, Yoshihiro K, Haskó G, and Pacher P. Simple quantitative detection of mitochondrial superoxide production in live cells. *Biochem Biophys Res Commun* 358: 203–208, 2007.
7. O'Brien WJ, Heimann T, and Rizvi F. NADPH oxidase expression and production of superoxide by human corneal stromal cells. *Mol Vis* 15: 2535–2543, 2009.

8. Pendyala S, Gorshkova IA, Usatyuk PV, He D, Pennathur A, Lambeth JD, Thannickal VJ, and Natarajan V. Role of Nox4 and Nox2 in hyperoxia-induced reactive oxygen species generation and migration of human lung endothelial cells. *Antioxid Redox Signal* 11: 747–764, 2009.
9. Robinson KM, Janes MS, Pehar M, Monette JS, Ross MF, Hagen TM, Murphy MP, and Beckman JS. Selective fluorescent imaging of superoxide *in vivo* using ethidium-based probes. *Proc Natl Acad Sci USA* 103: 15038–15043, 2006.
10. Souvannakitti D, Nanduri J, Yuan G, Kumar GK, Fox AP, and Prabhakar NR. NADPH oxidase-dependent regulation of T-type Ca^{2+} channels and ryanodine receptors mediate the augmented exocytosis of catecholamines from intermittent hypoxia-treated neonatal rat chromaffin cells. *J Neurosci* 30: 10763–10772, 2009.

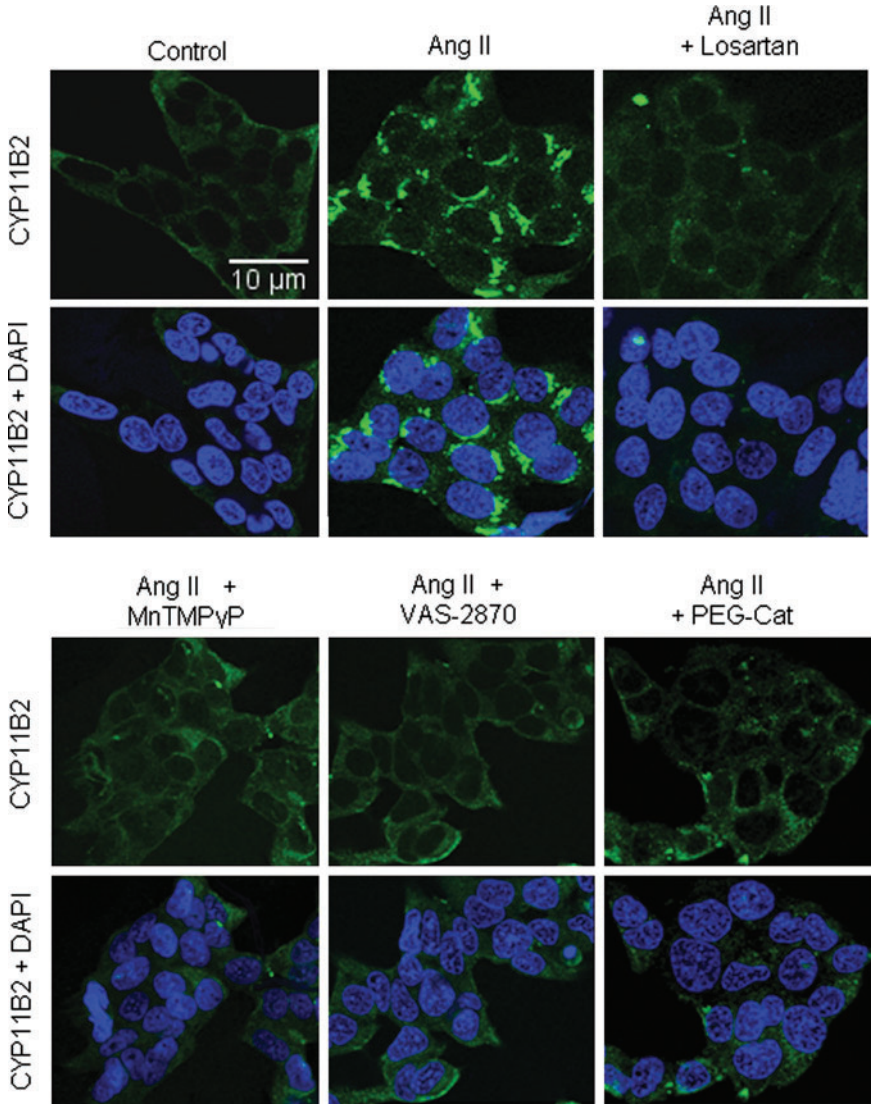

SUPPLEMENTARY FIG. S1. Immunocytochemical analysis of Ang II-evoked changes in CYP11B2 protein expression in human H295R cells. Cells grown in an eight-well glass slide chamber were treated with either vehicle (control) or Ang II (10 n*M* for 6 h) alone or in the presence of either antioxidant (MnTMPyP, 100 μM), H_2O_2 scavenger (PEG-Catalase, 350 U/ml), Nox inhibitor (VAS-2870, 10 μM), or AT_1R antagonist (losartan, 10 μM). Immunostaining for CYP11B2 was carried out with goat anti-CYP11B2 antibody as described in the Supplementary Methods section. Representative confocal images from six independent experiments are presented. Ang II, angiotensin II; CYP11B2, aldosterone synthase.

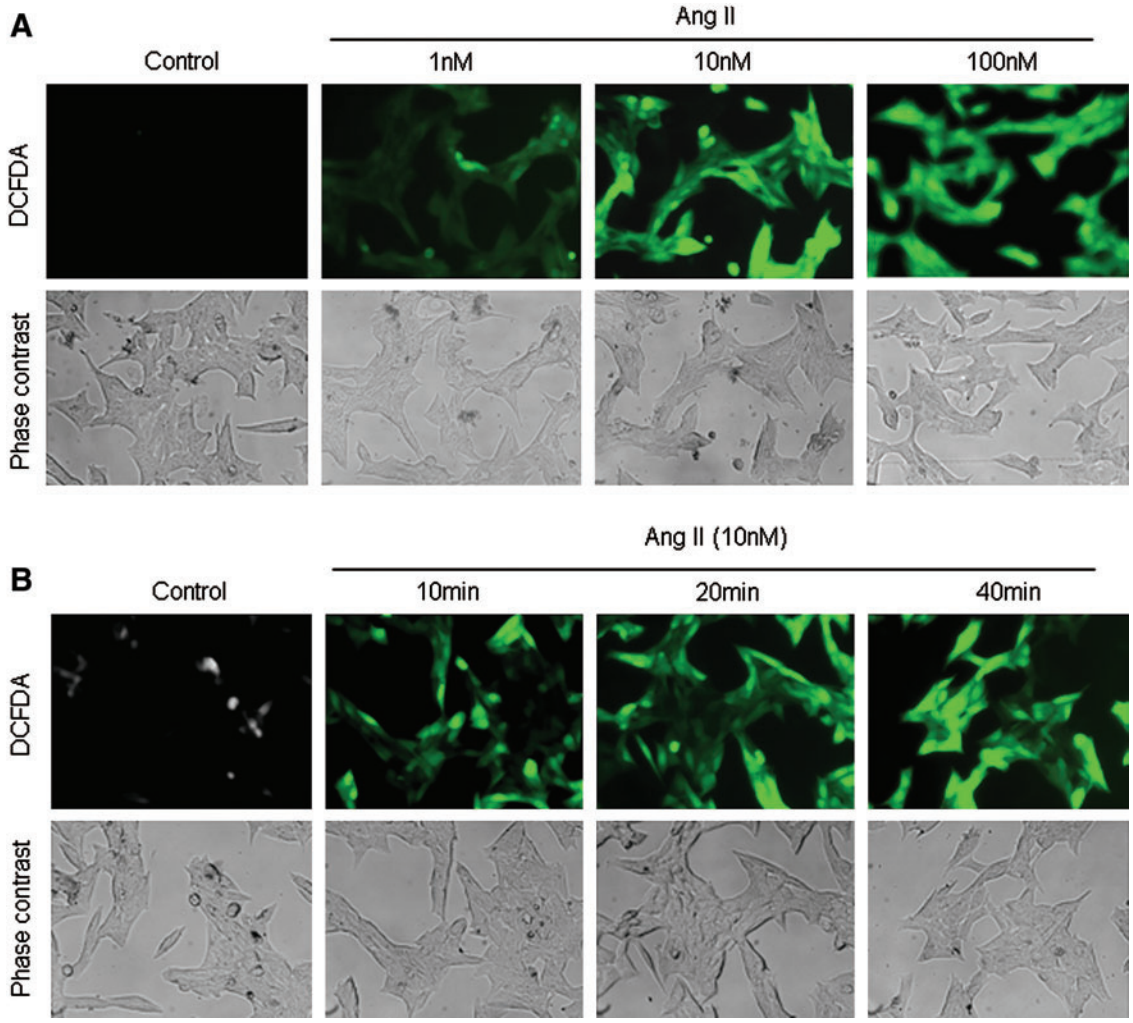

SUPPLEMENTARY FIG. S2. Induction of ROS generation by Ang II in human H295R cells. Cells were first loaded with DCFDA (5 μM, 30 min) and then challenged with increasing concentrations of Ang II (1, 10, and 100 nM) for 40 min **(A)** or challenged with Ang II (10 nM) for different durations (10, 20, and 40 min). **(B)** DCFDA oxidation was monitored by fluorescence microscopy. Representative images from six independent experiments are shown. ROS, reactive oxygen species; DCFDA, 6-Carboxy- 2′,7′-dichlorodihydrofluorescein diacetate.

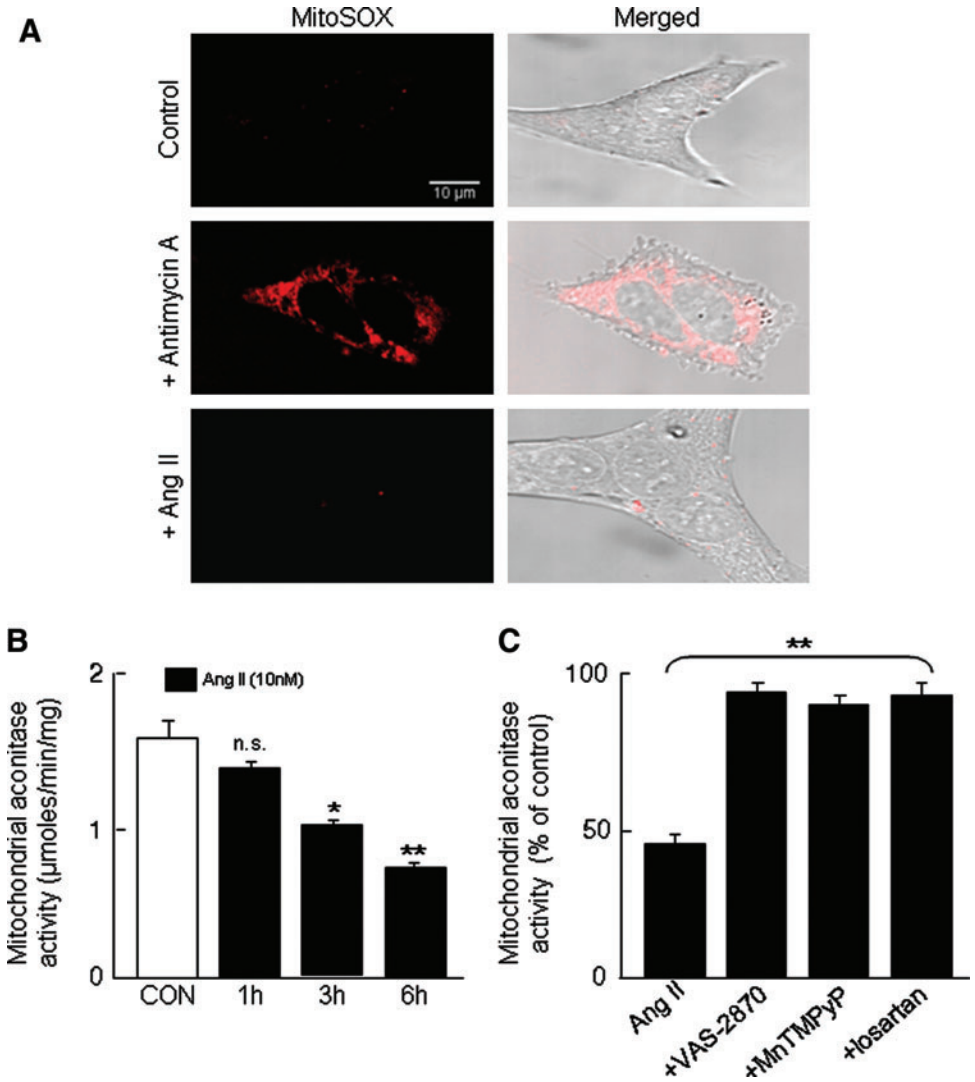

SUPPLEMENTARY FIG. S3. Effect of Ang II on mitochondrial ROS in H295R cells. Cells were treated with either Ang II (10 n*M*) or antimycin A (100 μM) for 40 min and then loaded with MitoSOX (1 μM) for 10 min. Intracellular MitoSOX Red-emitted fluorescence was visualized by immunofluorescence microscopy. Representative confocal images of H295R cells showing an increase in mitochondrial MitoSOX fluorescence after treatment with antimycin A (*middle panels*) but not with Ang II (*bottom panels*) are shown in **(A)**. Analysis of aconitase activity in the mitochondrial fraction of H295R cells treated with vehicle (CON) or Ang II (10 n*M*) for 1, 3, and 6 h **(B)**. Note that treatment with Ang II for 1 h has no significant effect on aconitase activity, whereas 3 and 6 h Ang II treatment induces a progressive decrease in the activity, suggesting an increase in mitochondrial ROS only after prolonged exposure to Ang II. Effects of VAS-2870 (20 μm), MnTMPyP (100 μm) and lasartan (10 μm) on Ang II (10 nM)-induced inhibition of mitochondrial aconitase activity **(C)** are shown.

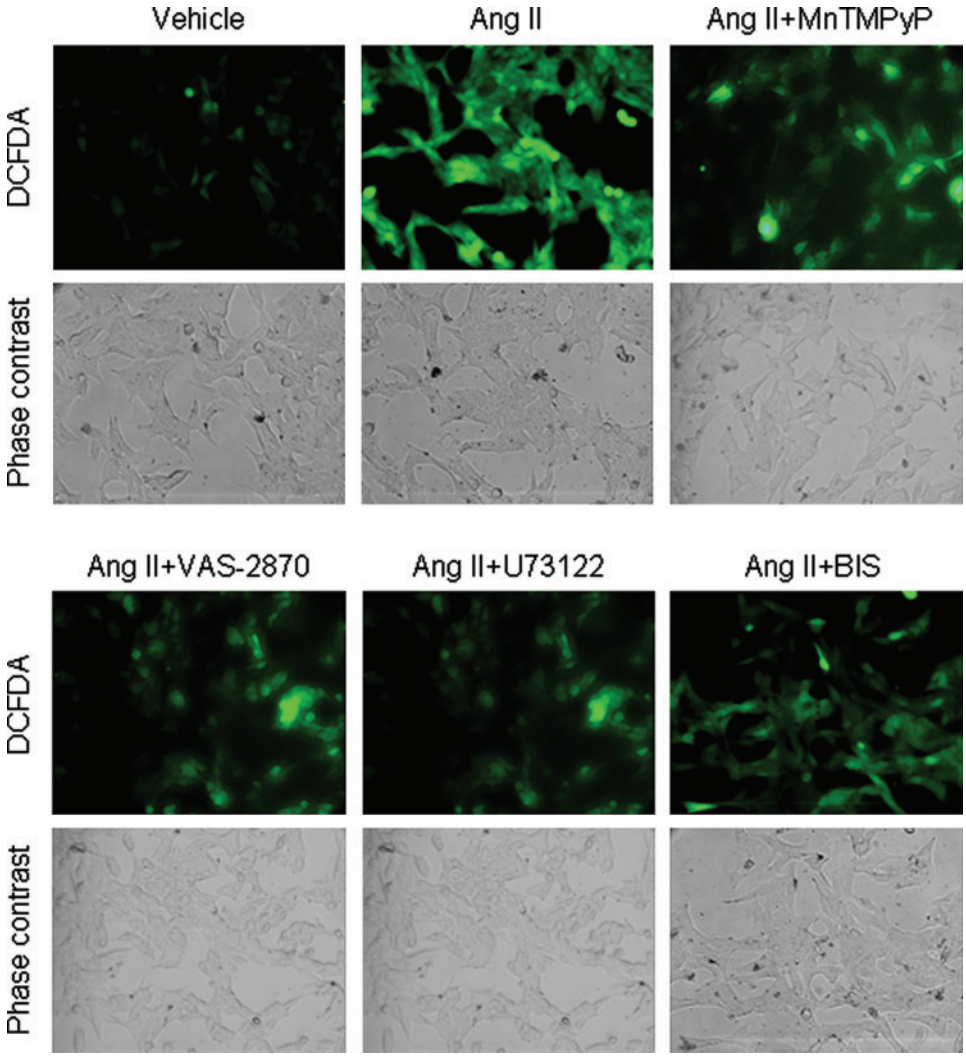

SUPPLEMENTARY FIG. S4. Effects of antioxidant, inhibitors of PLC, PKC, and Nox on Ang II-induced ROS generation in H295R cells. DCFDA (5 μM, 30 min) loaded cells were treated with Ang II (10 nM) for 40 min in the absence and presence of either antioxidant (MnTMPyP, 100 μM) or Nox inhibitor (VAS-2870, 20 μM) or PLC inhibitor (U73122, 10 μM) or PKC inhibitor (BIS, 10 μM). DCFDA oxidation was monitored by fluorescence microscopy. Representative images from six independent experiments are shown. PLC, phospholipase C; PKC, protein kinase C; BIS, Bisindolylmaleimide.

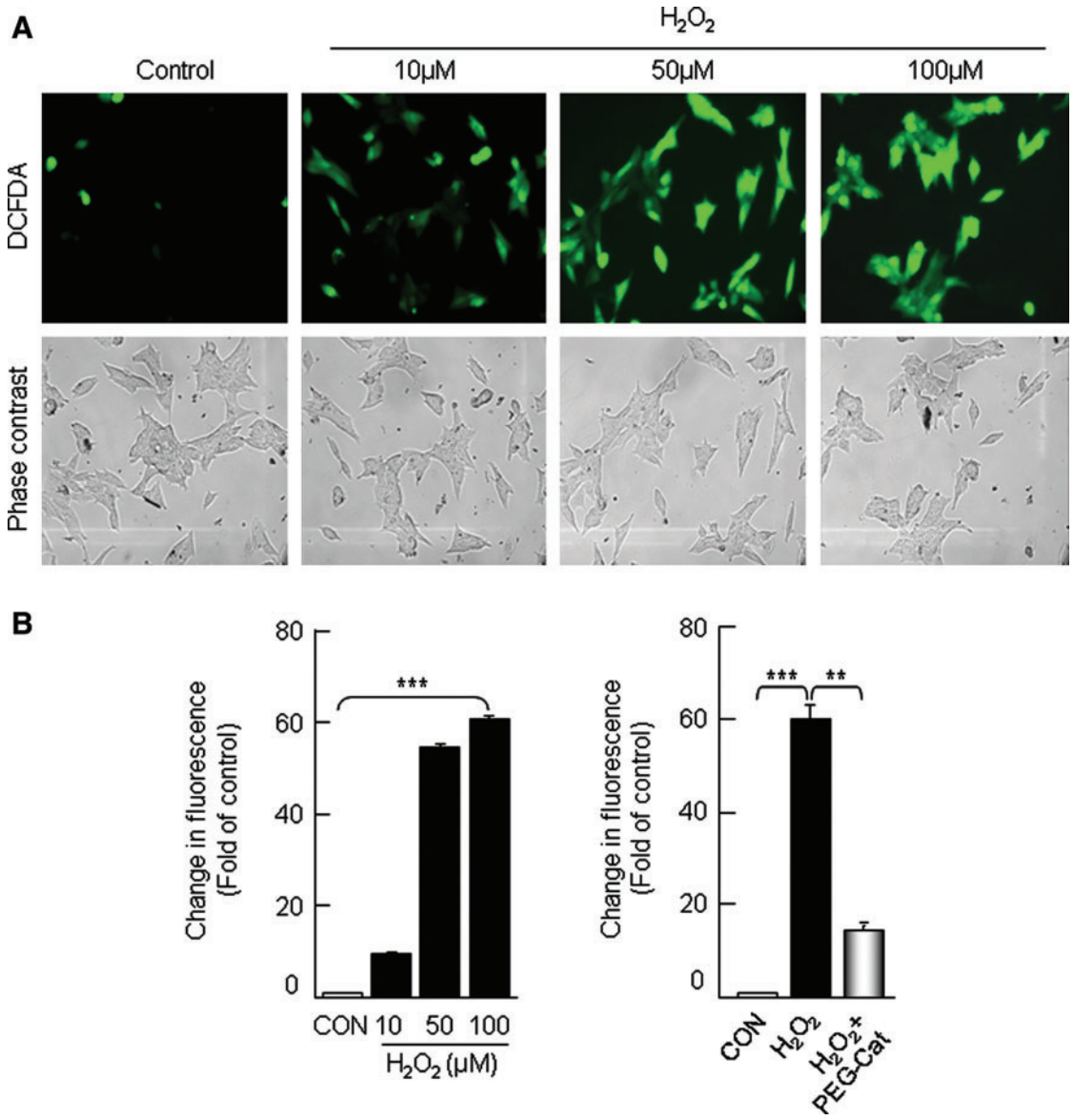

SUPPLEMENTARY FIG. S5. Effects of exogenous H_2O_2 on ROS generation in H295R cells. Cells were treated with H_2O_2 in the absence and presence of H_2O_2 scavenger (PEG-Cat, 350 U/ml) for 6 h at 37°C. Cells not treated with H_2O_2 served as control (CON). Effects of increasing concentration of H_2O_2 in the absence **(A)** and (**B**, left panel) and presence (**B**, right panel) of H_2O_2 scavenger (PEG-Catalase, 350 U/ml) on DCFDA fluorescence are shown. DCFDA oxidation was monitored by fluorescence microscopy. Representative images from six independent experiments are shown as mean ± SEM. $^{**}p < 0.01$ and $^{***}p < 0.001$.

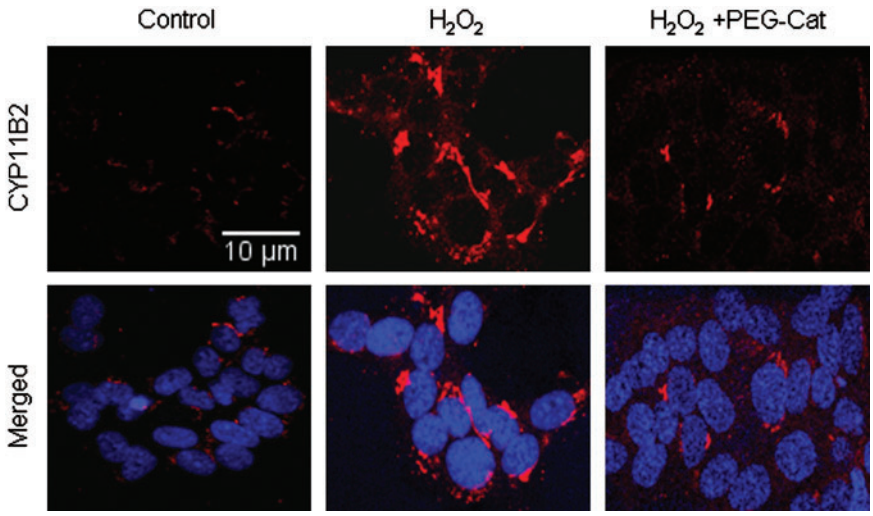

SUPPLEMENTARY FIG. S6. Effects of exogenous H_2O_2 on CYP11B2 expression in H295R cells. Cells grown in an eight-well glass slide chamber were treated with either vehicle (control) or H_2O_2 (50 μM for 6 h) alone or in the presence of H_2O_2 scavenger (PEG-Catalase, 350 U/ml). Immunostaining for CYP11B2 was carried out with goat anti-CYP11B2 antibody as described in the Supplementary Methods section. Representative confocal images from six independent experiments are presented.

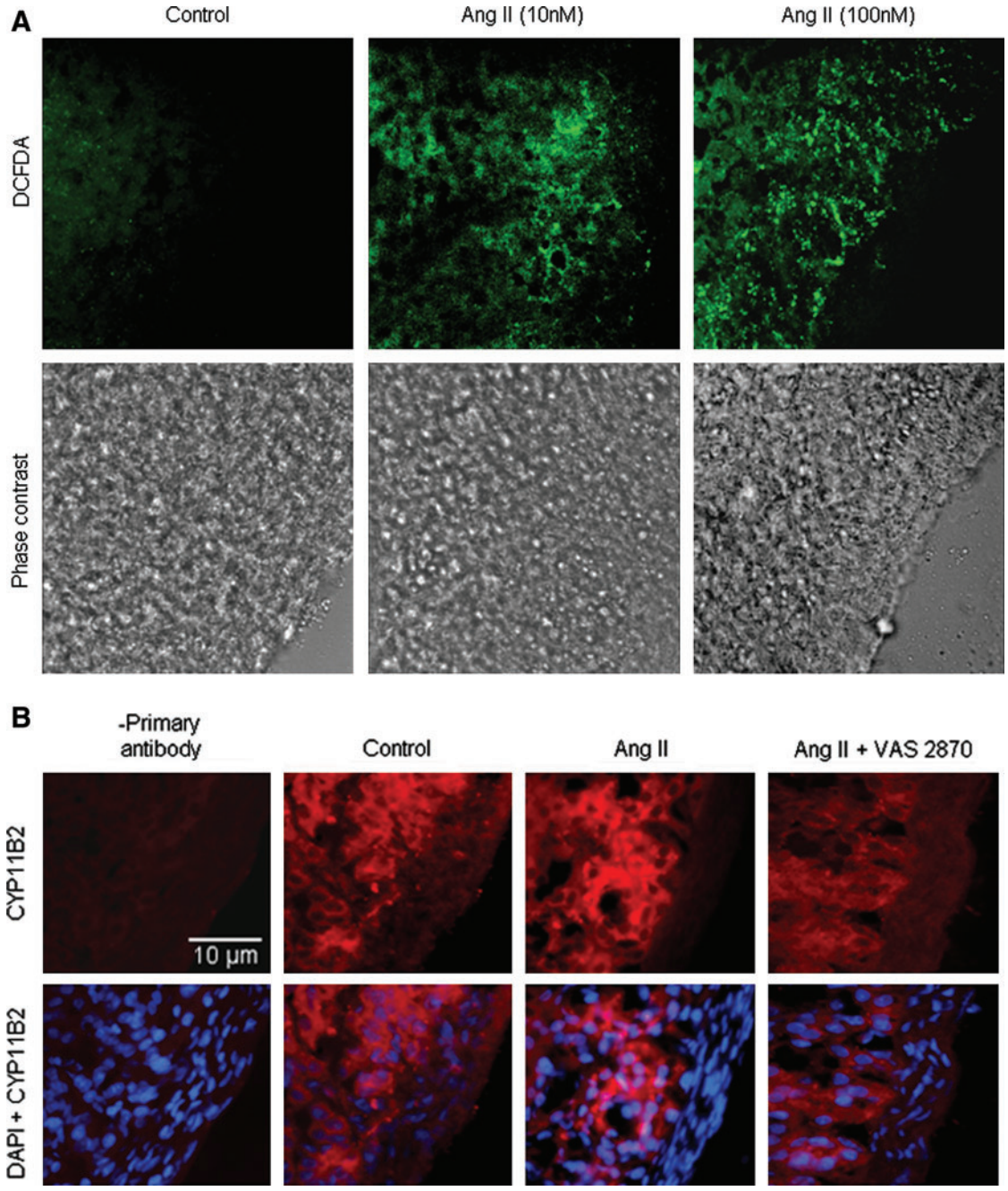

SUPPLEMENTARY FIG. S7. Induction of ROS generation and CYP11B2 by Ang II in rat adrenal cortex. Fresh unfixed rat adrenal cortical sections (20 μm) were loaded with DCFDA (10 μM, 30 min) and then challenged with either vehicle (control) or Ang II (10 and 100 nM) for 40 min **(A)**. DCFDA oxidation was monitored by fluorescence microscopy. Representative images from six independent experiments are shown. Elevation of CYP11B2-like immunoreactivity by Ang II in adrenal cortical sections containing zona glomerulosa is shown in **(B)**. Adrenal cortical sections (20 μm) were treated with vehicle (control) or Ang II (100 nM) or Ang II (100 nM) + Nox inhibitor (VAS-2870, 20 μM) for 6 h. Immunostaining for CYP11B2 was carried out with mouse anti-CYP11B2 antibody as described in the Supplementary Methods section. Representative confocal images from six independent experiments are presented.

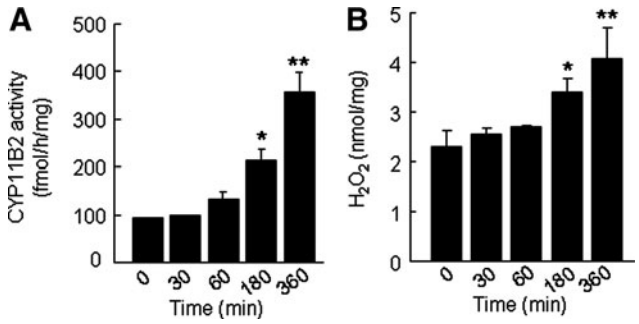

SUPPLEMENTARY FIG. S8. Time-dependent Ang II-induced changes in CYP11B2 activity and H_2O_2 formation in rat adrenal cortex. Fresh unfixed adrenal cortical sections (20 μm) were treated with Ang II (100 n*M*) for various durations as indicated. Changes in CYP11B2 activity **(A)** and H_2O_2 levels **(B)** evoked by Ang II are shown. Results derived from six independent experiments are presented as mean ± SEM. *$p < 0.05$ and **$p < 0.01$.

Supplementary Table S1. Primer Sequences Used for Real-Time Polymerase Chain Reaction Analysis

Gene	*Primer sequence 5′ to 3′*	*Reference*
hNox1	+1: TCACCAATTCCCAGGATTGAAGTGGATGGTC	(8)
NM_013955	−2: GACCTGTCACGATGTCAGTGGCCTTGTCAA	
hNox2	+1: GTCACACCCTTCGCATCCATTCTCAAGTCAGT	(8)
NM_174035	−2: CTGAGACTCATCCCAGCCAGTGA GGTAG	
hNox3	+1: GGATCGGAGTCACTCCCTTCGCTG	(8)
NM_015718	−2: ATGAACACCTCTGGGGTCAGCTGA	
hNox4	+1: CTGGAGGAGCTGGCTCGCCAACGAAG	(8)
NM_016931	−2: GTGATCATGAGGAATAGCACCAC CACCATGCAG	
hNox5	+1: GCAGGAGAAGATGGGGAGAT	(7)
NM_024505	−2: CGGAGTCAAATAGGGCAAAG	
rNox1	+1: CACTGTGGCTTTGGTTCTA	(10)
NM_053683	−2: TGAGGACTCCTGCAACTCCT	
rNox2	+1: GTGGAGTGGTGTGAATGC	(10)
NM_023965	−2: TTTGGTGGAGGATGTGATGA	
rNox3	+1: GACCCAACTGGAATGAGGA	(10)
NM_001004216	−2: ATGAACGACCCTAGGATCT	
rNox4	+1: GGGTGGCTTGTTGAAGTAT	(10)
NM_053524	−2: GGGGTGGCTTGTTGAAGTAT	
hCYP11B2	+1: AGATGCACCAGACCTTCCAG	(5)
NM_000498.3	−2: GTGGTCCTCCCAAGTTGTACC	
rCYP11B2	GGATGTCCAGCAAAGTCTC	(3)
NM_012538	ATTAGTGCTGCCACAATGC	
r18S	GTAACCCGTTGAACCCCATT	(10)
X_01117	CCATCCAATCGGTAGTAGCG	
hDuox1	5′-TTCACGCAGCTCTGTGTCAA-3′	(2)
NM_017434	5′-AGGGACAGATCATATCCTGGCT-3′	
hDuox2	5′-ACGCAGCTCTGTGTCAAAGGT-3′	(2)
NM_014080	5′-TGATGAACGAGACTCGACAGC-3′	